ORGANIC PROCESS RESEARCH & DEVELOPMENT
OPR&D

pubs.acs.org/OPRD

Article

Process Development and Optimization of Linagliptin Aided by the Design of Experiments (DoE)

Hailong Wang, Kai Chen, Biyue Lin, Jingping Kou, Lijun Li, Shuming Wu, Shouzhu Liao, Guodong Sun, Junwen Pu, Hua Yang,* and Zhongqing Wang*

Cite This: *Org. Process Res. Dev.* 2022, 26, 3254−3264

Read Online

ACCESS | Metrics & More | Article Recommendations | Supporting Information

ABSTRACT: A design of experiments (DoE) approach was applied to the development and optimization of the manufacturing process to prepare linagliptin. DoE techniques such as a central composite face-centered design and a fractional factorial design were applied to obtain the critical process parameters and establish the optimal reaction conditions. With process-related impurities determined and successfully removed, a robust high-yielding and high-purity procedure was identified, which has been successfully demonstrated at a 100 g scale level to prepare the desired product in a 68% overall isolated yield and high-performance liquid chromatography (HPLC) purity of around 99.9%.

KEYWORDS: *linagliptin, process optimization, DoE, impurity control*

INTRODUCTION

Diabetes is a spiraling epidemic with a growing prevalence in adults aged 20−79 years. The total number of global patients with diabetes has increased to ∼537 million since 2000, covering more than 10% population nowadays.[1] Albeit chronic, diabetes is estimated to account for 6.7 million deaths in 2021.[1] Thus, the treatment of diabetes has gathered increasing attention in recent years. There are two major types of diabetes, and type 2 diabetes makes up over 90% of all diabetes. Linagliptin (**1**, Figure 1) is a highly specific, long-acting dipeptidyl peptidase-4 (DPP-4) inhibitor developed by Boehringer Ingelheim for the treatment of type 2 diabetes.[2] It showed better DPP-4 inhibition over vildagliptin, sitagliptin, saxagliptin, and alogliptin and was approved by the FDA in 2011.[3] Furthermore, linagliptin is the only DPP-4 inhibitor that does not require dose adjustment for patients with an impaired renal function and is, therefore, most frequently prescribed for these patients.[4]

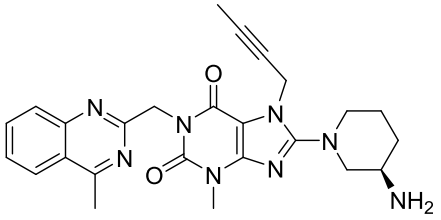

linagliptin (1)

Figure 1. Chemical structure of linagliptin (**1**).

As a result, considerable attention has been drawn to the synthesis of linagliptin, and a representative route was concluded after a literature review (Scheme 1): 8-bromo-3-methylxanthine (**2**) reacted with 2-butynyl bromide (BNB) to give *N*-alkylation compound **3**, which was then condensed with 2-(chloromethyl)-4-methylquinazoline (CMQ) in the presence of K_2CO_3 in DMF, providing1-(4-methylquinazolin-2-ylmethyl)-3-methyl-7-(2-butyn-1-yl)-8-bromoxanthine (**4**). Although treatment of **4** with unprotected 3-aminopiperidines under basic conditions gave rise to linagliptin (**1**) as the major product, it would be difficult to efficiently remove the regioisomer derived from the N-arylation of the 3-amine from the piperidine building block.[5] Alternatively, uses of *N*-protected aminopiperidines such as (*R*)-3-phthalimido piperidine,[6−8] (*R*)-3-azidopiperidine,[9] and (*R*)-3-Boc-aminopiperidine[2,10] have been well documented. In the case of phthalimide protection, the limitation was the overall low atom economy and the use of the expensive Nishimura catalyst for the synthesis of (*R*)-3-phthalimido piperidine.[8] Besides, (*R*)-3-azidopiperidine was not commercially available, which was not suitable for industrial synthesis. Thus, the synthetic route via (*R*)-3-Boc-aminopiperidine (RBP) seemed to be most suitable for large-scale industrial manufacture.

During our investigation of the synthetic route for linagliptin via (*R*)-3-Boc-aminopiperidine, two process-related impurities were detected (Figure 2), which could also be found in commercial drug products.[6] From the perspective of drug safety, process improvement and impurity minimization are of paramount importance. Since the initial introduction of Quality by Design (QbD), it has aroused much concern and interest from pharmaceutical regulatory authorities and the pharmaceutical industry. The concept that quality should be built by design rather than by a test has been embraced by the

Received: July 21, 2022
Published: November 16, 2022

https://doi.org/10.1021/acs.oprd.2c00230
Org. Process Res. Dev. 2022, 26, 3254−3264

Scheme 1. Representative Route of Linagliptin (1)[a]

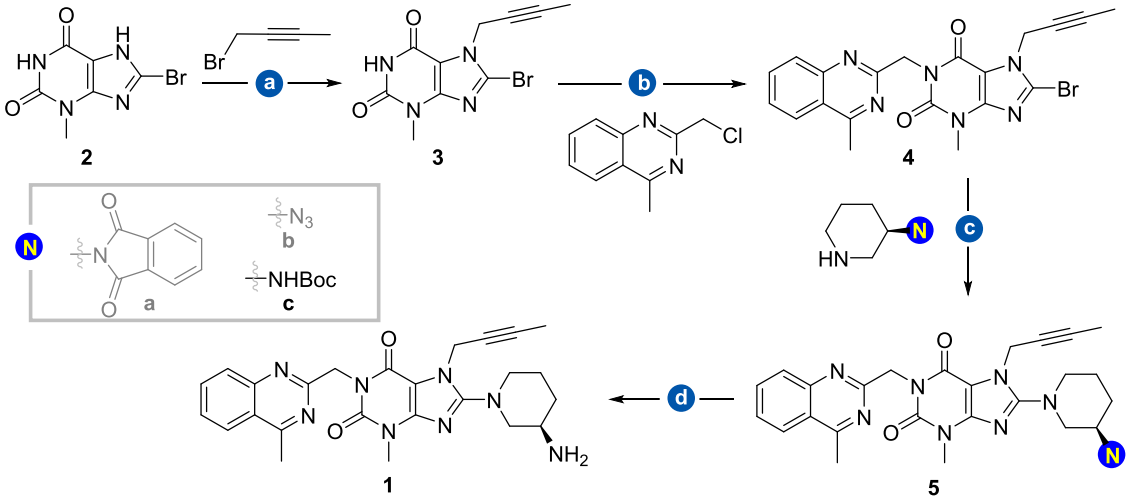

[a]Conditions: (a) *N*,*N*-Dimethylformamide (DMF), *N*,*N*-diisopropylethylamine (DIPEA), room temperature, and 86%; (b) DMF, K_2CO_3, room temperature, and 75%; (c) (*R*)-3-Boc-aminopiperidine, DMF, K_2CO_3, 75 °C, and 88%; (d) trifluoroacetic acid (TFA), dichloromethane (DCM), purified by flash column chromatography, and 91%.

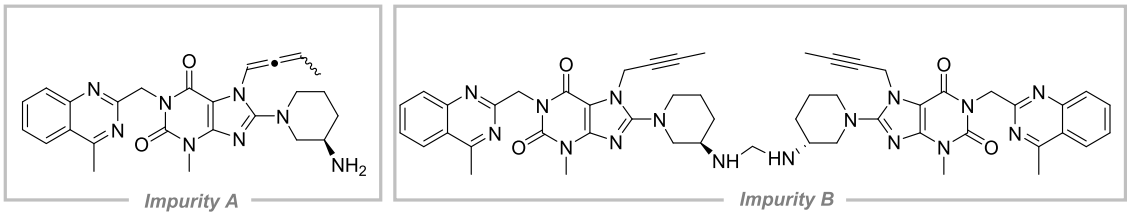

Figure 2. Process-related impurities of linagliptin (**1**).

pharmaceutical industry. Adoption of QbD during the development of drug substances was encouraged by regulatory agencies.[11] Noticeably, the design of experiments (DoE) is an extremely valuable and powerful tool for the development of active pharmaceutical ingredients (APIs) based on the concept of QbD. It can be used in early process development when the best conditions are not yet obvious and is a useful tool to resolve optimization issues in a timely manner.[12] To develop a robust process for industrial production and achieve high quality for further commercialization, we opted to use this DoE approach to help us improve the development efficiency and provide a fundamental basis for the understanding of the process in the early process development.

RESULTS AND DISCUSSION

Preparation of *N7*-Substituted Xanthine (3, Step 1). The first step in the original synthetic route involved a base-promoted *N*-alkylation of 8-bromoxanthine (**2**) with 2-butynyl bromide to afford 3-methyl-7-(2-butyn-1-yl)-8-bromoxanthine (**3**). The reaction was performed with *N*,*N*-dimethylformamide (DMF) as a solvent overnight, and then the reaction solution was poured into water to yield compound **3** as a water-insoluble solid product. Although DMF is one of the preferred polar aprotic solvents for a range of chemical transformations, the recovery of DMF from water is still a remarkable challenge. Moreover, DMF might be reactive toward a wide variety of substances, which may bring unexpected hazards to the products.[13] To find an ideal solvent for this process, different solvents were screened, including toluene, isopropanol, acetone, water, and acetonitrile. To our delight, acetonitrile was found to be optimal. After being heated at 80 °C for 12 h, typically more than 96% product was observed (by the HPLC area percentage). Compared with the previous procedures, using acetonitrile as a solvent could simplify the manufacturing process as the *N*-alkylation product **3** was able to be crystallized from this solvent. In addition, DIPEA could also be easily separated from **3**, considering DIPEA·HBr is quite soluble in acetonitrile.[14]

After the preliminary selection of the reaction condition, a DoE approach was then planned to better understand the most important factors affecting the residual starting material **2**, so as to minimize the impurity generated in the reaction process and thus optimize the robustness of the unit operation. Minitab statistical analysis software 20 (Minitab LLC) was used for the experimental design and statistical analysis. Five different factors: solvent volume, temperature, reaction time, and stoichiometry of BNB and DIPEA were considered as potentially significant parameters. A pre-DoE work was performed to define the ranges, as listed in Table 1. With the above data in hand, a fractional design (also called screening DoE) was generated with a set of eight experiments plus three three center points replicates[15,16] to identify the significant parameters (Table S1). Parallel experiments were carried out with a Mettler Toledo EasyMax 102 Basic Synthesis Workstation. The single response was the residual starting material **2**, ranging from 1 to 13% over the experimental space, confirming that the parameters and the selected ranges were meaningful. Stepwise regression[17] was performed to analyze the data. Clearly, the analysis of the variance (ANOVA) for the above screening DoE showed that

https://doi.org/10.1021/acs.oprd.2c00230
Org. Process Res. Dev. 2022, 26, 3254−3264

Table 1. Overview of DoE Factors in the Screening for Step 1[a]

factor	unit	range
acetonitrile	mL/g	10−16
BNB	equiv	1.0−1.3
temperature	°C	50−80
time	h	8−20
DIPEA	equiv	1.1−1.5

[a]0.05 equiv of tetrabutylammonium bromide (TBAB) was added.

the *p*-value of the model was 0.006 (Table S2), which meant the model was significant and effective. To avoid losing important parameters, the *p*-value threshold was set at 0.15 in the screening DoE. A half-normal plot (Figure 3) based on the preliminary analysis of the screening DoE revealed that the stoichiometry of BNB (variable B) was the most critical factor impacting the reaction conversion. The stoichiometry of DIPEA (variable E) and the interaction of variables B and E were also significant, while other variables were comparably less significant. It should be noted that the *p*-value of the lack of fit (LOF) and the curvature were 0.018 and 0.019, which underscored the complexity of the system and the need to utilize response surface methods (RSM) to secure a more definitive model of the data.[18,19]

To further understand the critical factors and build a model to control and predict the response variable, a central composite face-centered design (CCF), as a representative response surface method, was then implemented to evaluate the impacts of temperature[20] and the stoichiometry of DIPEA and BNB on the reaction conversion (Table S3). Although the temperature was not determined to be a significant factor in the screening DoE, typically, a higher temperature is in favor of reaching a higher conversion. Therefore, we took temperature again into account in the RSM DoE for a complete conversion. The reaction time and solvent volumes were fixed at 12 h and 12 V, respectively. A set of 18 experiments were carried out to develop a model of the response surface. The design and the reaction conversions from these experiments are shown in Table S4. Analysis of variance testing showed that the model was significant and effective (*p*-value < 0.05), and the LOF was not significant, which means the model fits the data. We also found that the stoichiometry of BNB (variable B), the stoichiometry of DIPEA (variable E), the square of variable E, and the interaction between variables B and E were significant factors (*p*-value < 0.05), as shown in Table S5. The results shown in the main effects plot[21] of the residue of **2** (Figure 4a) suggested a positive correlation between the stoichiometry of BNB and the reaction conversion. Hence, the highest reaction conversion in our experimental range was observed with 1.20 equiv of BNB. Interestingly, although an increased amount of DIPEA could also promote conversion, the trend was reversed when DIPEA was charged with more than 1.27 equiv Moreover, increasing the reaction temperature could also favor the reaction conversion, and a negative linear correlation could be observed between reaction temperature and residual starting material **2**. The contour plot of residual starting material **2** vs DIPEA and BNB illustrated in Figure 4b demonstrates the dependence of the residue of **2** on the amounts of BNB (variable B) and DIPEA (variable E) at the optimal level of temperature (variable C). Similar plots were obtained at different temperatures as variable C was kept in the model. To improve the reaction conversion, the stoichiometry of BNB and temperature were expected to be increased. Per the model, the predicted optimal conditions were 1.20 equiv of BNB and 1.27 equiv of DIPEA at 80 °C. The obtained best reaction conditions were further confirmed by four replicates, which had a mean value of residual starting material **2** at 0.8% within a 95% confidence interval (Table S6). The results indicate that the obtained model was suitable and the predictions were credible. Furthermore, a scale-up reaction in batch (100 g of starting material **2**) was carried out; the HPLC test showed that 0.91% of the raw material remained, and the expected product **3** was obtained in a 94% isolated yield and 99.17% purity (by HPLC).

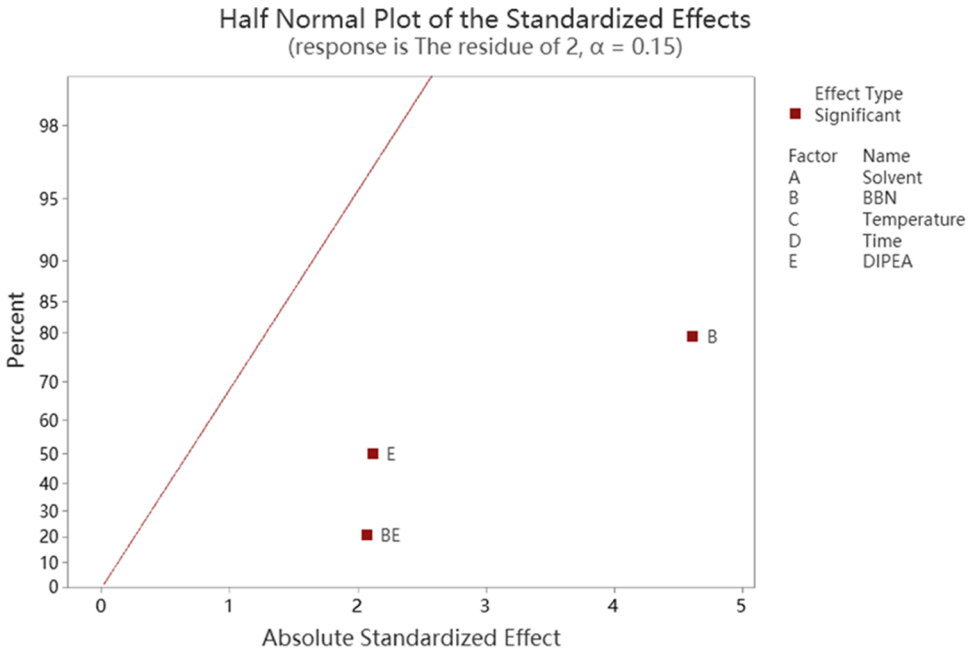

Figure 3. Half-normal plot showing the stoichiometry of BNB (B) and DIPEA (E) and their interaction effect (BE).

https://doi.org/10.1021/acs.oprd.2c00230
Org. Process Res. Dev. 2022, 26, 3254−3264

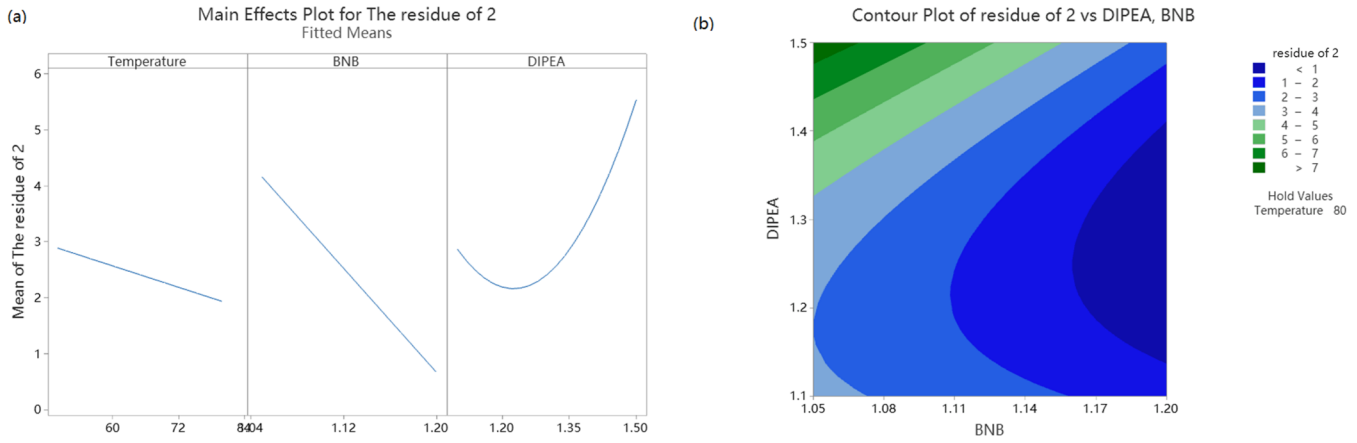

Figure 4. Plot for equiv of DIPEA, equiv of BNB, and temperature in the residual starting material **2**. (a) Plot of main effects on the reaction conversion and (b) contour plot of residual starting material **2** vs DIPEA and BNB.

Preparation of *N*1,7-Disubstituted Xanthine (4, Step 2). The next step in the synthetic route was *N*1-alkylation of compound **3** by 2-(chloromethyl)-4-methylquinazoline (CMQ) in the presence of K_2CO_3, providing *N*1,7-disubstituted xanthine **4**. In the original synthetic routes, DMF or *N*-methylpyrrolidone (NMP) was chosen as the solvent. Considering that DMF is incompatible with a wide variety of substrates,[13] especially inorganic bases, NMP seemed to be the preferred solvent for commercial production. With categorical variables defined, we then proceeded with the DoE studies to obtain optimal parameters.

Results from exploratory experiments indicated that the major impurities remaining in the reaction mixture were the residues of **3** and CMQ. To maximize reaction conversion, a Screening DoE was first implemented to identify critical factors for controlling the residue of **3**. As listed in Table 2, five parameters including (1) stoichiometry of CMQ, (2) stoichiometry of K_2CO_3, (3) reaction time, (4) temperature, and (5) stoichiometry of NMP were investigated. A half-fraction fractional factorial design was generated, and a set of 16 experiments plus 4 replicates of the center point were carried out (Table S7). Analysis of the half-normal plot determined the amount of K_2CO_3, CMQ, and reaction time to be statistically significant to the measured response (residual starting material **3**) (Figure 5). However, reaction temperature and solvent volumes were less important, and they were set at 60 °C and 8 mL/g for future experiments, respectively. A significant curvature (*p*-value 0.000, <0.05) was observed in this model, and the LOF test was also significant (*p*-value 0.016, <0.05, Table S8), which indicated that the reliable model must include at least one quadratic term. The CCF design was again performed to further evaluate the impacts of three important factors, including K_2CO_3, CMQ, and reaction time. The ranges of the selected parameters were based on the results of the earlier screening design.

Table 2. Overview of DoE Factors in the Screening for Step 2[a]

factor	unit	range
CMQ	equiv	1.0−1.2
K_2CO_3	equiv	0.5−2.0
time	h	4−14
temperature	°C	50−90
NMP	mL/g	8−14

[a]0.1 equiv of TBAB was added.

A set of 17 experiments were conducted to examine the effects of K_2CO_3, CMQ, and reaction time on the reaction conversion (Table S9). ANOVA of these experiments (Table S10) clearly inferred that the RSM model was significant and effective (*p*-value of the model was 0.000, <0.05, while the *p*-value of LOF was 0.190 > 0.05). The main effects plot for the residue of **3** (Figure 6a) showed the tendency line for each factor, and it suggested that the stoichiometry of K_2CO_3, rather than that of CMQ, was the most important factor influencing the reaction conversion. Figure 6b shows how the residue of **3** could be controlled by the stoichiometry of K_2CO_3 and CMQ. However, the impact of K_2CO_3 loading is much more significant than other reaction parameters, as indicated in Figure 6a. As such, when K_2CO_3 reached an optimum loading (i.e., >1.75 equiv), a complete conversion of the starting material would be observed. At this point, it seemed that CMQ had no impact on the critical quality attributes of this reaction. In contrast, when the stoichiometry of K_2CO_3 was lower than 1.5 equiv, the dependence of reaction conversion on CMQ loading could still be observed. Therefore, it could be concluded from the figures that 1.80 equiv of K_2CO_3 and 1.13 equiv of CMQ were the optimal parameters for the reaction conversion, as either increasing or decreasing the loading would lead to a lower reaction conversion. In addition, a higher reaction conversion could be observed with a longer reaction time, and the optimal reaction time was chosen to be 14 h in the experimental space. With the optimal parameters in hand, four verification experiments were then carried out, and only 0.15% of the residual starting material **3** was detected by HPLC within a 95% confidence interval (Table S11). A 100 g scale experiment was also performed, affording the expected product **4** in an 86% yield and 99.31% purity (by HPLC). As expected, an experimental space for the control of residual **3** by optimizing the amount of K_2CO_3, CMQ, and reaction time was built. The specification of residual **3** was defined as less than 1% (by the HPLC area percentage) in the experimental space, and less than 0.5% was advised in the control space.

Preparation of *N*-Boc Linagliptin (5, Step 3). The subsequent step was the preparation of *N*-Boc linagliptin **5** via a nucleophilic substitution reaction of (*R*)-3-Boc-amino-piperidine (RBP) and 1,7-disubstituted xanthine **4** in the

https://doi.org/10.1021/acs.oprd.2c00230
Org. Process Res. Dev. 2022, 26, 3254−3264

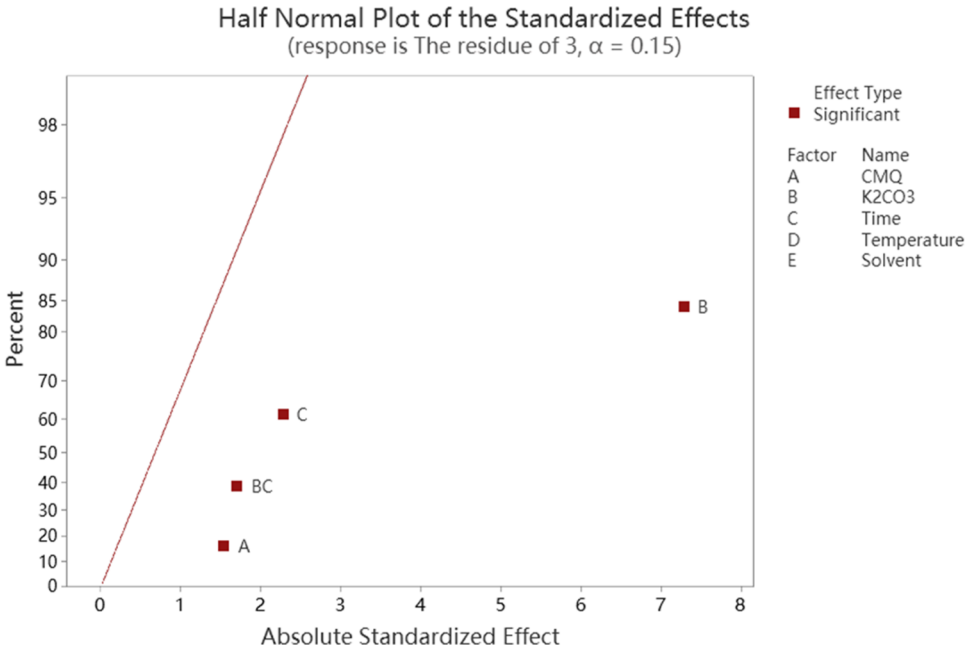

Figure 5. Half-normal plot showing significant effects of equiv of K_2CO_3 (B), reaction time (C), their interaction effect (BC), and equiv of CMQ.

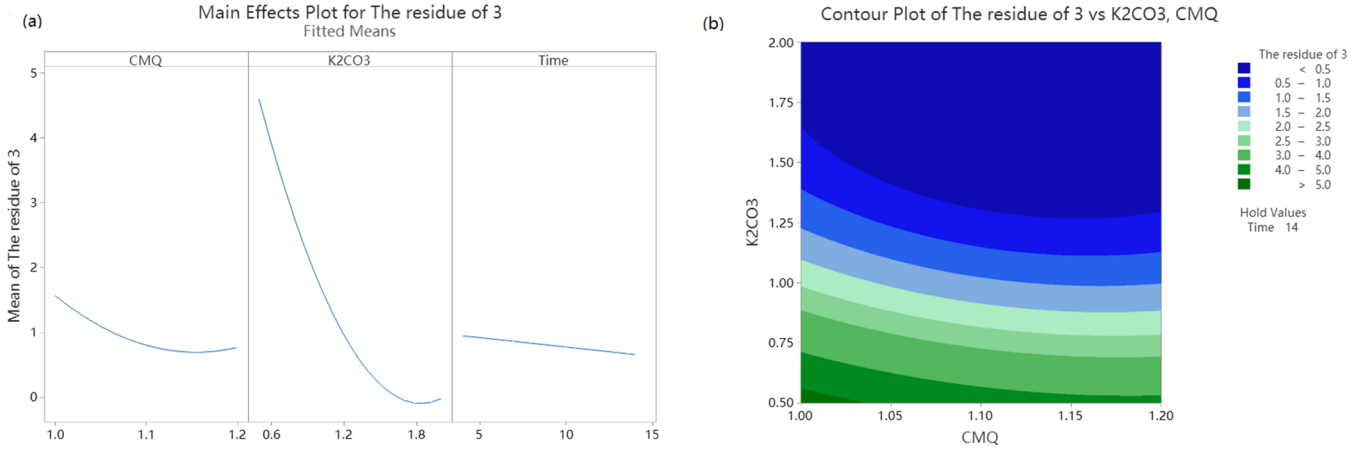

Figure 6. Plot for equiv of K_2CO_3 and CMQ on the residual starting material **3**. (a) Plot of main effects on the reaction conversion and (b) contour plot of residual starting material **3** vs K_2CO_3 and CMQ.

Scheme 2. Plausible Pathway for the Formation of Impurities A and C[22,23]

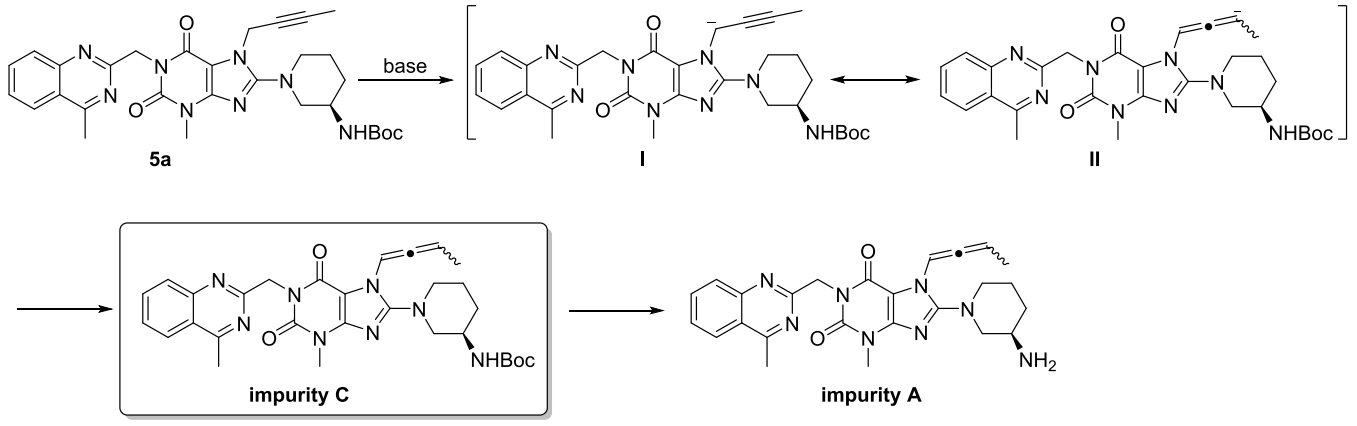

presence of K_2CO_3. Instead of DMF in the original synthetic route, NMP was again used as the solvent. Results of exploratory experiments showed that in NMP at 75 °C, the reaction proceeded smoothly in the presence of 2 equiv of

https://doi.org/10.1021/acs.oprd.2c00230
Org. Process Res. Dev. 2022, 26, 3254−3264

K_2CO_3, but an allene impurity was observed in both the reaction mixture and the product *N*-Boc linagliptin **5**. A further single-factor experiment found that the level of the allene byproduct (impurity **C**) seemed to correlate with the feeding amount of K_2CO_3 (Table S12). Presumably, impurity **C** was formed via a base-promoted isomerization of *N*-Boc linagliptin **5** (Scheme 2). It should be noted that impurity **C** undergoes hydrolytic cleavage of *tert*-butyloxycarbonyl amine to afford impurity **A**, which could be detected in the commercial linagliptin product at a 0.2% level.[6] For the safety of the patients, APIs with higher purities and with impurities purged as much as possible are welcomed. To achieve the high-purity intermediate, impurity **C** was supposed to be significantly purged to an undetectable level (the limit of detection was 0.025%). If successful, the final deprotection step leading to linagliptin would not be burdened with input-related impurities.

Considering that impurity **C** was formed *via* base-mediated alkyne−allene isomerization, different bases such as KOH and Na_2CO_3 were screened for this nucleophilic substitution reaction (Table 3). To our delight, impurity **C** was not detected when using 2 equiv of Na_2CO_3, which was very promising for further studies. Thus, DoE was planned to implement to control the allene impurity and the residue of **4**. Reaction time, stoichiometry of Na_2CO_3, volumes of NMP, and stoichiometry of RBP were selected as potentially significant parameters that would affect the generation of allene impurity and residue of **4**. The typical ranges were defined by exploratory experiments, and are listed in Table 4.

Table 3. Screen of the Alternative Bases Used in the Preparation of 5

base	K_2CO_3[a]	Na_2CO_3[b]	KOH[C]
allene impurity	0.31	ND	0.70

[a]Conditions: **4** (2 g), NMP (16 mL), K_2CO_3 (1.2 g, 2 equiv), 23 h, and 90 °C. [b]Conditions: **4** (2 g), NMP (16 mL), Na_2CO_3 (0.9 g, 2 equiv), 23 h, and 90 °C. [C]Conditions: **4** (2 g), NMP (16 mL), KOH (1.0 g, 4 equiv), 21 h, and 100 °C.

Table 4. Overview of DoE Factors in the Screening for Step 3

factor	unit	range
temperature	°C	70−100
time	h	12−16
Na_2CO_3	equiv	0.5−2.0
NMP	mL/g	6−12
RBP	equiv	1.00−1.12

To evaluate the influence of these five factors, a half-fraction factorial design was used in which two responses, starting material conversion and allene impurity formation, were tracked. A 16 experiment half-factorial design plus three center point replicates were run in the experimental space (Table S13). From the results of ANOVA (Tables S14 and S15), the *p*-value of the model were all significant (0.000 and 0.002, <0.05), which meant the models were significant and effective. In terms of factor selection for RSM studies, the *p*-value threshold was defined as 0.10 in case more than three factors were included, based on the concept of "factor sparsity".[24] The half-normal plot indicated that the significant factors influencing the allene impurity formation were observed to be temperature (variable A), the stoichiometry of RBP (variable C), and their interaction (Figure 7a), while except variables A and C, reaction time (variable B) and the interaction of variables A and B were also crucial to the starting material conversion (Table S14 and Figure 7b).

According to the results of screening DoE, the temperature was the most significant factor influencing the generation of allene impurity. The range of the temperature was narrowed to 70−90 °C to control the formation of such an impurity. The CCF design was carried out, and a set of 17 experiments were performed (Table S16) to identify optimal ranges for three important parameters: reaction temperature, reaction time, and the amount of RBP. Based on the results from the RSM DoE (Table S16), an allene impurity could hardly be detected under this temperature range. Therefore, good control over the allene impurity was achieved, and we no longer chose the level of the allene impurity to be a response in the RSM study.

ANOVA of the RSM design (Table S17) identified reaction temperature and the amount of RBP as the most significant parameters (*p*-value = 0.000), influencing the residual starting material **4** and the assay of **5**. The square of temperature, the square of RBP, and the interaction between temperature and RBP were of relatively low statistical significance (*p*-value range from 0.007 to 0.043, Tables S17 and S18). The reaction time was confirmed as an insignificant parameter. An overlapping contour plot built from the statistical model obtained is presented in Figure 8, and the goals defined were the residual of **4** less than 0.5% and an assay yield of **5** higher than 98%. The white area of the overlapping contour plot represents the optimal process conditions where the defined criteria for the residual of **4** and assay yield were all achieved. On the basis of the overlapping contour plot, optimized conditions were defined to be using 1.16 equiv of RBP and 1 equiv of Na_2CO_3 in NMP at 82 °C for 16 h. Since higher equiv of RBP also involves additional work to remove excess reagents at the end of the reaction, particularly during scale-up, the amount of RBP was slightly adjusted to be 1.09 equiv according to the response surface studies. With the optimal parameters in hand, four verification experiments were then carried out (Table S19). It was found that the residual starting material **4** was less than 0.3%, the assay yield was higher than 98%, and no impurity **C** was detected in four replicates. A 100 g scale experiment was then carried out using 1.09 equiv of RBP at 82 °C for 16 h, and the assay yield of **5** was 98.77%. Analysis of the reaction did not reveal any generation of an allene impurity. After work-up, *N*-Boc linagliptin **5** was obtained in a 96% yield and 99.47% purity (by HPLC) with no allene impurity detected (the limit of detection was 0.025%).

Preparation of Linagliptin 1 and Impurity Control. The final step in the workflow was the deprotection of the *N*-Boc group of **5** to give the final product **1**. Although the TFA-mediated conditions were well studied in the original process, they would not be employed in this study considering the introduction of an *N*-trifluoroacetyl linagliptin impurity,[25] high cost, and environmental hazard.[26] Then, alternative catalyst systems such as HCl and $ZnCl_2$ were then examined (Table S20). To our delight, HCl seemed to be optimal as it is cost-efficient and environmentally friendly. Although this conversion was efficient and convenient, two impurities **D** and **E** were observed. As shown in Scheme 3, the formation of impurity **D** should be attributed to an electrophilic addition of

https://doi.org/10.1021/acs.oprd.2c00230
Org. Process Res. Dev. 2022, 26, 3254−3264

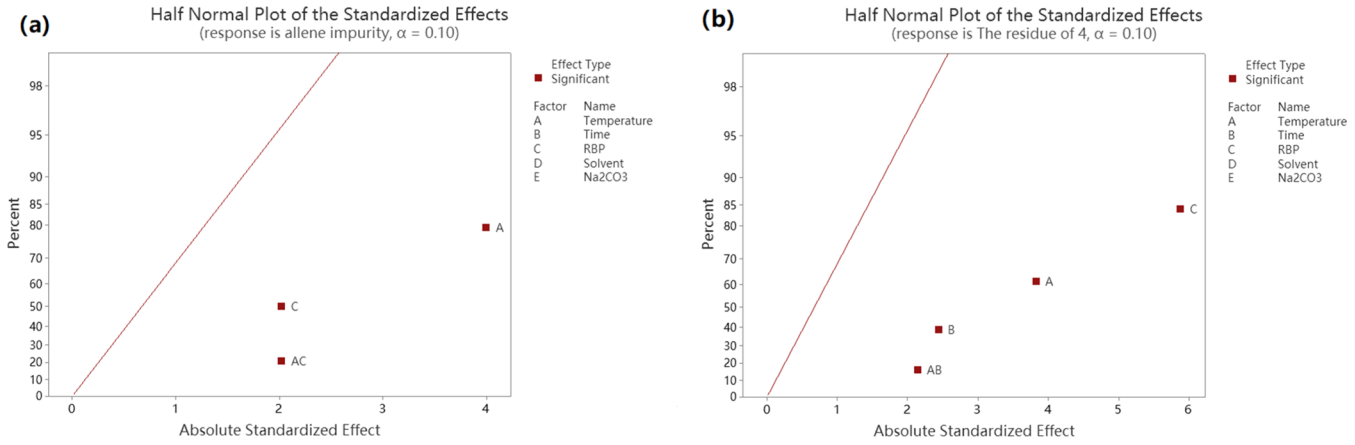

Figure 7. Half-normal plot. (a) Allene impurity formation and (b) residual starting material **4**.

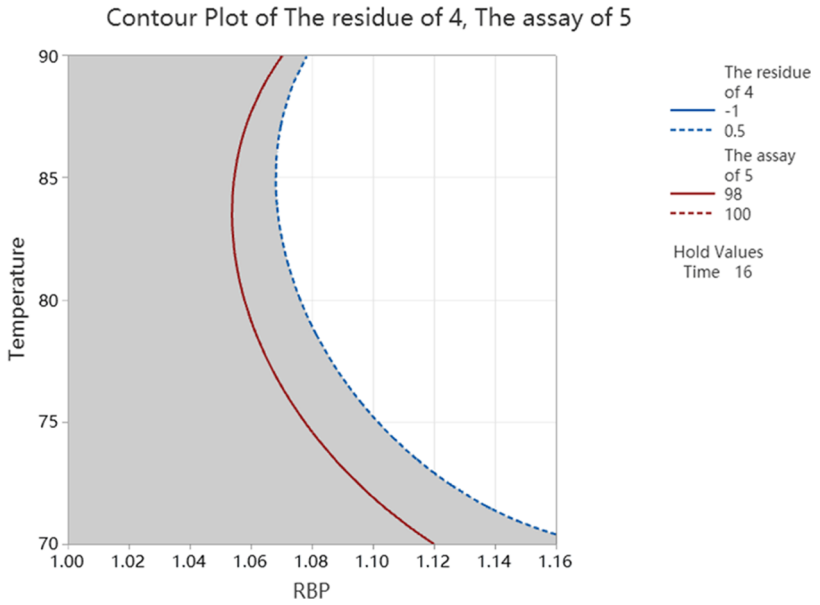

Figure 8. Reaction overlapping contour plot.

Scheme 3. Plausible Pathways for the Formation of Impurities D and E

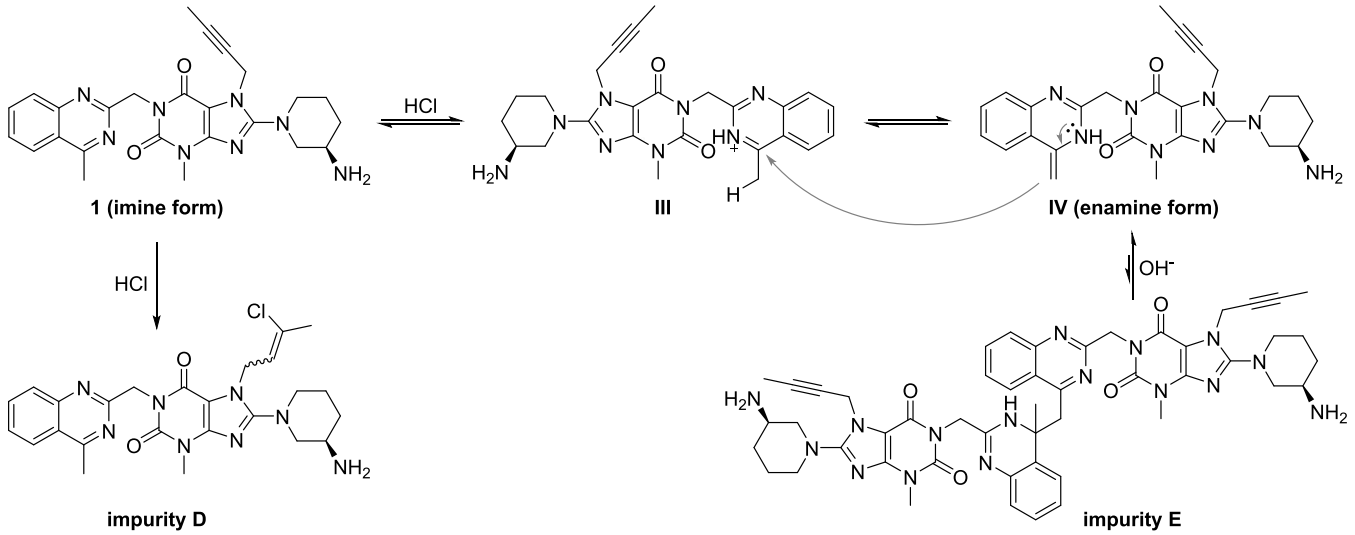

https://doi.org/10.1021/acs.oprd.2c00230
Org. Process Res. Dev. 2022, 26, 3254−3264

HCl to the alkyne moiety of linagliptin, while acid-catalyzed dimerization led to the formation of impurity **E**.

Control of Impurity D. As the formation of impurity **D** was irreversible, strict control of its formation was requisite with a limit of less than 0.1%. Initial optimization of the reaction conditions suggested that temperature was a critical factor for the formation of impurity **D**. As shown in Table 5,

Table 5. Optimization of the Reaction Temperature in the Deprotection Step[a]

exp no	temp (°C)	**1** (%)[b]	impurity **D** (%)[b]	impurity **E** (%)[b]
1	−15	60	nd[c]	40
2	−5	58	nd[c]	42
3	10	55	nd[c]	45
4	30	63	0.2	36

[a]Reaction conditions: **2** (3.0 g), DCM (15 mL), conc. HCl (12 M, aq. 5 mL), for 5 h. [b]HPLC yield. [c]nd = not detected.

the reaction resulted in an almost complete conversion of reactants at the temperature ranging from −15 to 30 °C in 5 h. It should be noted that impurity **D** was below the limit of detection (LOD was 0.05%) when the reaction temperature was lower than 10 °C. Although the assay of impurity **E** was about 40%, it could be easily converted to linagliptin under basic conditions in the postprocessing steps (vide infra).

Control of Impurity E. After deprotection, excess aqueous NaOH (7.5 M) was added to neutralize HCl and maintain the pH value above 11. It was found that impurity **E** could be converted to linagliptin **1** completely at 60 °C in 4 h. Unfortunately, a 0.3% level of impurity **B** was observed, which was plausibly derived from the nucleophilic substitution reaction between DCM and linagliptin. In this case, alternative solvents such as tetrahydrofuran (THF), toluene, and isopropyl acetate should be considered. The thermally stable toluene seemed to be the optimal solvent, which could offer good solubility for the reactants and effectively avoid the nucleophilic substitution reaction with linagliptin under reflux (Table S21). Therefore, the postprocessing steps were carried out as follows (Scheme 4): (1) extracting the protonated linagliptin and impurity **E** with water; (2) neutralizing excess HCl and maintaining a basic condition by adding aqueous NaOH; (3) adding toluene as a solvent and tetrabutylammonium bromide (TBAB) as a phase-transfer catalyst, and then refluxing the toluene/water solution for 4 h; (4) separating the toluene phase from the hot mixture, followed by evaporation and condensation; and (5) recrystallizing linagliptin from isopropanol. In the end, the linagliptin product was obtained in high purity with around 99.9% HPLC purity, without impurities **A** and **B** observed above the detection level (LOD was 0.009%).

CONCLUSIONS

In summary, a design of experiments approach was applied to the development and optimization of the manufacturing processes to prepare linagliptin, enabling a robust process capable of synthesizing products with excellent yields and high purities suitable for further development (Scheme 5). Using DoE techniques, critical process parameters were identified, and the optimal reaction conditions were established for each step. Process-related impurities were removed successfully, with less than 0.1% level. Moreover, the process was successfully scaled up to 100 g of starting material **2**, leading to the desired product in a 68% overall isolated yield with HPLC purity of around 99.9%, while marketed linagliptin (purity 99.35%) contained 0.21% of impurity **A** and 0.08% of impurity **B**.[27] This work also highlights the strength of DoE for efficient optimization of processing parameters at the early development of pharmaceutical production.

EXPERIMENTAL SECTION

Unless otherwise noted, all reagents and solvents were commercially available and used as purchased without further purification. NMR spectra were recorded with a Bruker Avance 400 spectrometer in the solvents indicated. Chemical shifts were reported in units (ppm) relative to tetramethylsilane and with solvent resonance as the interior standard. Coupling constants were reported in Hz with multiplicities denoted as singlet (s), doublet (d), triplet (t), quartet (q), dd (doublet of doublets); m (multiples), etc. HRMS was performed on a Fourier transform ion cyclotron resonance mass spectrometer. Parallel experiments were performed on a Mettler Toledo EasyMax 102 Basic Synthesis Workstation.

8-Bromo-3-methyl-1*H*-purine-2,6(3*H*,7*H*)-dione (3). Acetonitrile (1200 mL), BNB[28] (66.5 g), TBAB (6.6 g), DIPEA (67.4 g), and **2** (100.0 g) were charged into a 2000 mL reaction kettle. Then, the mixture was stirred at 80 °C for 12 h. Upon reaction completion (the residue of **2** was less than 2%, determined by HPLC), the slurry was cooled to 20 ± 5 °C, stirred for 2 h, and the precipitated solid was filtered, washed

Scheme 4. Manufacturing Process for the Final Step

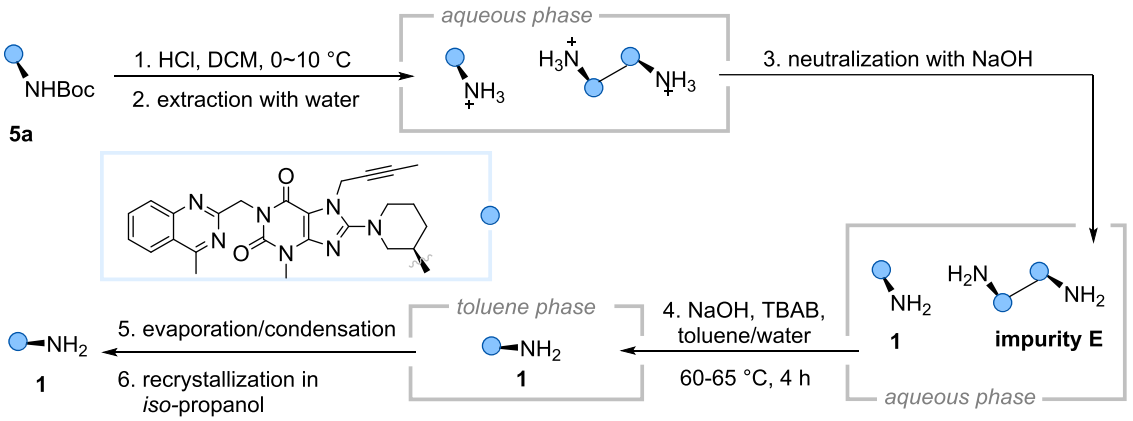

https://doi.org/10.1021/acs.oprd.2c00230
Org. Process Res. Dev. 2022, 26, 3254−3264

Scheme 5. Optimized Manufacturing Process of Linagliptin (1)

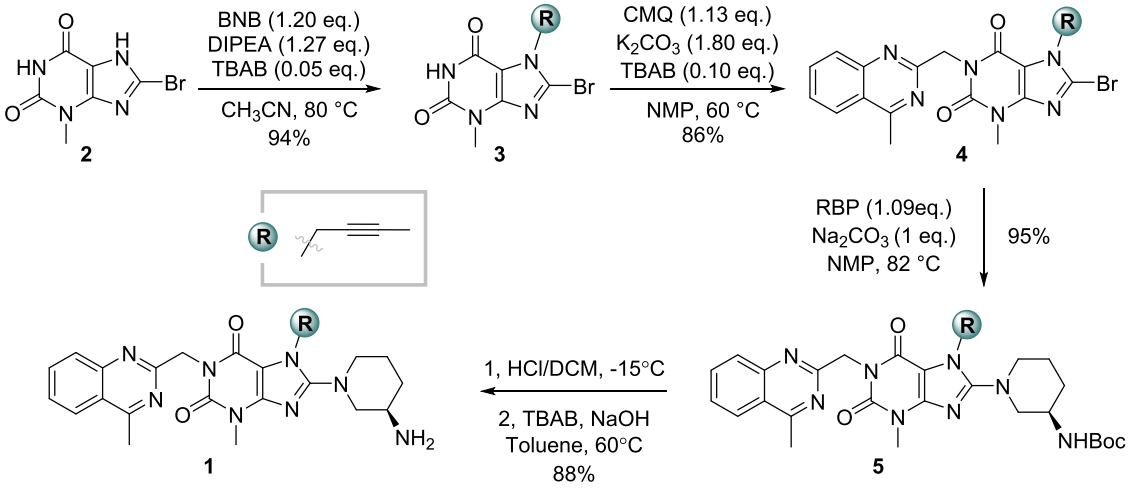

with acetonitrile, and finally dried at 70 °C under a vacuum for 8 h to give **3** as an off-white powder (115 g, 94% yield, 99.17% HPLC purity). HRMS (ESI) *m*/*z*: $[M + H]^+$ calculated for $C_{10}H_9BrN_4O_2$ 296.9982; found 296.9984. ^{1}H NMR (400 MHz, DMSO-d_6): δ 11.31 (s,1H), 5.05 (d, *J*= 2.2 Hz, 2H), 3.31 (s, 3H), 1.79 (s, 3H). ^{13}C NMR (400 MHz, DMSO-d_6): δ 153.79, 150.43, 149.14, 127.65, 108.07, 81.79, 72.29, 36.46, 28.48, 2.93.

8-Bromo-7-(but-2-yn-1-yl)-3-methyl-1-((4-methylquinazolin-2-yl)methyl)-1*H*-purine-2,6(3*H*,7*H*)-dione (4). **3** (100.0 g), CMQ (73.4 g), TBAB (10 g), K_2CO_3 (83.3 g), and methyl-2-pyrrolidinone (800 mL) were added to a 3000 mL reaction kettle. The mixture was stirred at 60 °C for 14 h. Upon reaction completion (the residue of **3** was less than 1%, determined by HPLC), the slurry was cooled to 15 °C and aged for 1−2 h to induce crystallization. After adding water (1600 mL) slowly, the temperature of the solution was kept at 25−35 °C. Then, the resulting suspension was agitated for 2 h and filtered. The filter cake was then washed with water (150 mL) to give **4** as the crude product.

To a 2000 mL reaction kettle, the above crude product, acetonitrile (600 mL), and water (200 mL) were charged. The solution was stirred at 85 °C for 2 h. Then, the reaction solution was cooled to 50 °C and stirred for 0.5 h. At last, the temperature was reduced to 30 °C and stirred for another 0.5 h. The reaction solution was filtered. The resulting filter cake was washed with acetonitrile/water (150 mL V/V = 3:1) and dried at 70 °C under a vacuum for 8 h to provide **4** (130 g, 86% yield, 99.31% HPLC purity) as a light yellow powder. HRMS (ESI) *m*/*z*: $[M + H]^+$ calculated for $C_{20}H_{17}BrN_6O_2$ 453.0669; found 453.0682. ^{1}H NMR (400 MHz, DMSO-d_6): δ 8.26 (d, *J* = 8.2 Hz, 1H), 7.91 (t, *J* = 7.6 Hz, 1H), 7.81 (d, *J* = 8.4 Hz, 1H), 7.68 (t, *J* = 7.6 Hz, 1H), 5.34 (s, 2H), 5.11 (d, *J* = 1.9 Hz, 2H), 3.43 (s, 3H), 2.88 (s, 3H), 1.78 (s, 3H). ^{13}C NMR (400 MHz, DMSO-d_6): δ 168.97, 160.37, 153.30, 150.55, 148.97, 147.99, 134.11, 128.42, 127.83, 127.21, 125.73, 122.49, 107.65, 81.91, 72.29, 45.73, 36.63, 29.56, 21.53,2.95

(*R*)-*tert*-Butyl(1-(7-(but-2-yn-1-yl)-3-methyl-1-((4-methylquinazolin-2-yl)methyl)-2,6-dioxo-2,3,6,7-tetrahydro-1*H*-purin-8-yl)piperidin-3-yl)carbamate (5). To a 3000 mL reaction kettle, **4** (100.0 g), RBP (48.4 g), Na_2CO_3 (23.5 g), and methyl-2-pyrrolidinone (780 mL) were charged. The solution was stirred at 80 °C for 16 h. Upon reaction completion (the residue of **4** was less than 0.5%, determined by HPLC), toluene (100 mL) was added and stirred for 0.5 h. Then, water (1500 mL) was added slowly at 75−85 °C. The resulting solution was stirred for 0.5 h at 75−85 °C, and then cooled to 20−30 °C and stirred for another 1 h. The resulting suspension was filtered. The filter cake was washed with 1500 mL of water and then transferred to a 1000 mL reaction kettle with 380 mL of EtOH and 760 mL of water. The mixture was stirred at 65 °C for 2 h, then stirred at 50 °C for 0.5 h, and finally stirred at 30 °C for another 0.5 h. The solution was filtered, and the resulting filter cake was washed with 100 mL of water and dried at 70 °C under a vacuum for 12 h to furnish product **5** (120 g, 95.3% yield, 99.47% HPLC purity) as a light yellow solid. HRMS (ESI) *m*/*z*: $[M + H]^+$ calculated for $C_{30}H_{36}N_8O_4$ 573.2932; found 573.2950. ^{1}H NMR (400 MHz, DMSO-d_6): δ 8.24 (d, *J* = 8.2 Hz, 1H), 7.92 (t, *J* = 7.5 Hz, 1H), 7.81 (d, *J* = 8.3 Hz, 1H), 7.68 (t, *J* = 7.5 Hz, 1H), 6.99 (d, *J* = 7.5 Hz, 1H), 5.32 (s, 2H), 4.87 (s, 2H), 3.68 (d, *J* = 11.1 Hz, 1H), 3.59 (d, *J* = 11.3 Hz, 2H), 3.39 (s, 3H), 3.04 (t, *J* = 10.4 Hz, 1H), 2.87 (m, 4H), 1.85 (t, *J* = 10.1 Hz, 2H), 1.76 (s, 3H), 1.68 (m, 1H), 1.47−1.32 (m, 10H). ^{13}C NMR (400 MHz, DMSO-d_6): δ 168.78, 160.92, 155.71, 154.89, 153.25, 150.89, 149.02, 147.50, 134.02, 127.85, 127.09, 125.68, 122.46, 103.32, 81.08, 77.81, 73.68, 54.04, 49.63, 46.41, 45.53, 35.37, 29.54, 29.39, 23.13, 21.52, 3.02.

(*R*)-8-(3-Aminopiperidin-1-yl)-7-(but-2-yn-1-yl)-3-methyl-1-((4-methylquinazolin-2-yl)methyl)-1*H*-purine-2,6(3*H*,7*H*)-dione (1). To a 100 mL reactor, **5** (100.0 g) and dichloromethane (700 mL) were charged. Then, the solution was cooled to −15 °C, and concentrated hydrochloric acid (12 M, 150 mL) was added slowly under stirring. Upon reaction completion (the residue of **5** was less than 0.5%, determined by HPLC), water (70 mL) was added to separate the organic layer. The resulting aqueous phase was collected and extracted with dichloromethane (100 mL) twice.

After that, toluene (400 mL), TBAB (10.0 g), and sodium hydroxide solution (7.5 M, 150 mL) were added. Then, the reaction mixture was stirred at 60−65 °C. Once the reaction was completed (the residue of impurity **E** was less than 0.5%, determined by HPLC), the organic layer was separated and washed with water (600 mL) at 55−65 °C. The organic phase was distilled under reduced pressure to remove the toluene solvent completely. After that, isopropanol (1000 mL) was added and stirred at 80 °C until the solute was completely dissolved. Then, activated carbon (5 g) was added and then

https://doi.org/10.1021/acs.oprd.2c00230
Org. Process Res. Dev. 2022, 26, 3254−3264

removed through hot filtration. The hot solution was cooled to 25−30 °C and aged for 1 h. The purer crystals precipitated were collected by filtration, washed with isopropanol (150 mL), and dried at 60 °C under a vacuum for 12 h, affording target product **1** as a light yellow powder (72.4 g, 88% yield, 99.98% HPLC purity). HRMS (ESI) m/z: $[M + H]^+$ calculated for $C_{25}H_{28}N_8O_2$ 473.2408; found 473.2429. ^{1}H NMR (400 MHz, DMSO-d_6): δ 8.23 (d, J = 8.3 Hz, 1H), 7.91 (t, J = 7.6 Hz, 1H), 7.81 (d, J = 8.4 Hz, 1H), 7.67 (t, J = 7.6 Hz, 1H), 5.32 (s, 2H), 4.89 (s, 2H), 3.67 (dd, J = 21.8, 11.6 Hz, 2H), 3.39 (s, 3H), 3.28 (d, J = 48.3 Hz, 2H), 3.05-2.96 (m, 1H), 2.87 (s, 3H), 2.85−2.73 (m, 2H), 1.87 (dd, J = 12.5,3.2 Hz, 1H), 1.72 (s, 4H), 1.67−1.58 (dt, J = 13.4, 7.1 Hz, 1H), 1.27−1.18 (m, 1H). ^{13}C NMR (400 MHz, DMSO-d_6): δ 168.74, 160.95, 156.10, 153.19, 150.89, 149.00, 147.70, 133.98, 127.81, 127.05, 125.64, 122.43, 103.15, 81.08, 73.71, 57.55, 49.51, 47.22, 45.51, 35.45, 33.17, 29.36, 23.24, 21.50, 3.01.

■ ASSOCIATED CONTENT

Supporting Information

The Supporting Information is available free of charge at https://pubs.acs.org/doi/10.1021/acs.oprd.2c00230.

Detail reaction data and ^{1}H, ^{13}C NMR spectra, and HPLC chromatography for compounds **3**, **4**, **5**, and **1** (PDF)

■ AUTHOR INFORMATION

Corresponding Authors

Hua Yang − *College of Chemistry and Chemical Engineering, Central South University, Changsha 410083, P. R. China;* orcid.org/0000-0002-5518-5255; Email: Hyangchem@csu.edu.cn

Zhongqing Wang − *State Key Laboratory of Anti-Infective Drug Development, Sunshine Lake Pharma Co., Ltd., Dongguan 523871, P. R. China; School of Pharmacy, Xiangnan University, Chenzhou 423000 Hunan, P. R. China; HEC Research and Development Center, HEC Pharm Group, Dongguan 523871, P. R. China;* orcid.org/0000-0001-5194-4157; Email: Wangzhongqing@hec.cn

Authors

Hailong Wang − *College of Chemistry and Chemical Engineering, Central South University, Changsha 410083, P. R. China; State Key Laboratory of Anti-Infective Drug Development, Sunshine Lake Pharma Co., Ltd., Dongguan 523871, P. R. China; HEC Research and Development Center, HEC Pharm Group, Dongguan 523871, P. R. China*

Kai Chen − *College of Chemistry and Chemical Engineering, Central South University, Changsha 410083, P. R. China;* orcid.org/0000-0003-1012-0383

Biyue Lin − *State Key Laboratory of Anti-Infective Drug Development, Sunshine Lake Pharma Co., Ltd., Dongguan 523871, P. R. China; HEC Research and Development Center, HEC Pharm Group, Dongguan 523871, P. R. China*

Jingping Kou − *HEC Research and Development Center, HEC Pharm Group, Dongguan 523871, P. R. China*

Lijun Li − *HEC Research and Development Center, HEC Pharm Group, Dongguan 523871, P. R. China*

Shuming Wu − *State Key Laboratory of Anti-Infective Drug Development, Sunshine Lake Pharma Co., Ltd., Dongguan 523871, P. R. China; HEC Research and Development Center, HEC Pharm Group, Dongguan 523871, P. R. China*

Shouzhu Liao − *State Key Laboratory of Anti-Infective Drug Development, Sunshine Lake Pharma Co., Ltd., Dongguan 523871, P. R. China; HEC Research and Development Center, HEC Pharm Group, Dongguan 523871, P. R. China*

Guodong Sun − *State Key Laboratory of Anti-Infective Drug Development, Sunshine Lake Pharma Co., Ltd., Dongguan 523871, P. R. China; HEC Research and Development Center, HEC Pharm Group, Dongguan 523871, P. R. China;* orcid.org/0000-0003-3785-7641

Junwen Pu − *HEC Research and Development Center, HEC Pharm Group, Dongguan 523871, P. R. China*

Complete contact information is available at: https://pubs.acs.org/10.1021/acs.oprd.2c00230

Notes

The authors declare no competing financial interest.

■ ACKNOWLEDGMENTS

This work was financially supported by the State Key Laboratory of Anti-Infective Drug Development (Sunshine Lake Pharma Co., Ltd.) (No. 2015DQ780357) and the Key-Area Research and Development Program of Guangdong Province (2022B1111050003).

■ REFERENCES

(1) *IDF Diabetes Atlas*, 10th ed.; International Diabetes Federation: Brussels, 2021.

(2) Eckhardt, M.; Langkopf, E.; Mark, M.; Tadayyon, M.; Thomas, L.; Nar, H.; Pfrengle, W.; Guth, B.; Lotz, R.; Sieger, P.; Fuchs, H.; Himmelsbach, F. 8-(3-(R)-Aminopiperidin-1-yl)-7-but-2-ynyl-3-methyl-1-(4-methyl-quinazolin-2-ylmethyl)-3,7-dihydropurine-2,6-dione (BI 1356), a Highly Potent, Selective, Long-Acting, and Orally Bioavailable DPP-4 Inhibitor for the Treatment of Type 2 Diabetes. *J. Med. Chem.* **2007**, *50*, 6450−6453.

(3) Thomas, L.; Eckhardt, M.; Langkopf, E.; Tadayyon, M.; Himmelsbach, F.; Mark, M. (R)-8-(3-Amino-piperidin-1-yl)-7-but-2-ynyl-3-methyl-1-(4-methyl-quinazolin-2-ylmethyl)-3,7-dihydro-purine-2,6-dione (BI 1356), a Novel Xanthine-Based Dipeptidyl Peptidase 4 Inhibitor, Has a Superior Potency and Longer Duration of Action Compared with Other Dipeptidyl Peptidase-4 Inhibitors. *J. Pharmacol. Exp. Ther.* **2008**, *325*, 175−182.

(4) Mikov, M.; Pavlović, N.; Stanimirov, B.; Đanić, M.; Goločorbin-Kon, S.; Stankov, K.; Al-Salami, H. DPP-4 Inhibitors: Renoprotective Potential and Pharmacokinetics in Type 2 Diabetes Mellitus Patients with Renal Impairment. *Eur. J. Drug. Metab. Pharmacokinet.* **2020**, *45*, 1−14.

(5) (a) Dong, W.; Huang, Y.; Su, S.; Sun, Y.; Zhang, P. Process for The Preparation of a Xanthine-based Compound. PCT Patent WO2016207364, 2016. (b) Haldar, P.; Muvva, V.; Prataprao, A. K.; Karri, V. K.; Taduri, B. P.; Birudaraju, V. N. Process for Preparation of Pure Linagliptin. U.S. Patent US9056112, 2015. (c) Fang, L.; Li, J.; Chen, Y.; Du, T.; Ge, L.; Wang, Z. Method for Simple Preparation of High-purity Linagliptin. Chinese Patent CN105541844, 2016.

(6) Ciancimino, C.; Tragni, M.; Vigo, D.; Piccolo, O. Intermediates and Processes for the Preparation of Linagliptin and Its Salts. PCT Patent WO2019219620, 2019.

(7) Cao, Y. H.; Zhang, H. J.; Wu, J.; Zhang, L.; Gao, X. Preparation of Intermediate for Synthesizing Linagliptin. Chinese Patent CN105801580, 2016.

(8) Pfrengle, W.; Pachur, T. Preparation of Chiral 8-(3-amino-piperidin-1-yl)xanthines. U.S. Patent US20060142310, 2006.

(9) Himmelsbach, F.; Langkopf, E.; Eckhardt, M.; Mark, M.; Maier, R.; Lotz, R. R. H.; Tadayyon, M. Preparation of 8-[3-aminopiperidin-1-yl]xanthines as Dipeptidylpeptidase-IV (DPP-IV) Inhibitors. U.S. Patent US7407955, 2008.

(10) (a) Chennamsetty, S. M. B.; Gharpure, M.; Zalte, Y.; Chavan, K.; Thombre, P. An Improved Process for the Preparation of Linagliptin. Indian Patent IN201621030017, 2018. (b) Suri, S.; Tanwar, P. M.; Mishra, K. S. An Improved Process for the Synthesis of Highly Pure Linagliptin along with New Polymorph and Novel Processes for Preparation of Various Polymorphs of Linagliptin. Indian Patent IN201611032051, 2018. (c) Joshi, N.; Verdia, J.; Pandya, J.; Kothadiya, S. An Improved Process for The Preparation of Linagliptin. Indian Patent IN2014MU01004, 2015.
(11) Cimarosti, Z.; Bravo, F.; Castoldi, D.; Tinazzi, F.; Provera, S.; Perboni, A.; Papini, D.; Westerduin, P. Application of the QbD Principles in the Development of the Casopitant Mesylate Manufacturing Process. Process Research Studies for the Definition of the Control Strategy of some Drug Substance-CQAs for Stages 2a, 2b, and 2c. *Org. Process Res. Dev.* **2010**, *14*, 805−814.
(12) Weissman, S. A.; Anderson, N. G. Design of Experiments (DoE) and Process Optimization. A Review of Recent Publications. *Org. Process Res. Dev.* **2015**, *19*, 1605−1622.
(13) Yang, Q.; Sheng, M.; Huang, Y. L. Potential Safety Hazards Associated with Using N,N-Dimethylformamide in Chemical Reactions. *Org. Process Res. Dev.* **2020**, *24*, 1586−1601.
(14) Anderson, N. G.; Ary, T. D.; Berg, J. L.; Bernot, P. J.; Chan, Y. Y.; Chen, C.-K.; Davies, M. L.; DiMarco, J. D.; Dennis, R. D.; Deshpande, R. P.; Do, H. D.; Droghini, R.; Early, W. A.; Gougoutas, J. Z.; Grosso, J. A.; Harris, J. C.; Haas, O. W.; Jass, P. A.; Kim, D. H.; Kodersha, G. A.; Kotnis, A. S.; LaJeunesse, J.; Lust, D. A.; Madding, G. D.; Modi, S. P.; Moniot, J. L.; Nguyen, A.; Palaniswamy, V.; Phillipson, D. W.; Simpson, J. H.; Thoraval, D.; Thurston, D. A.; Tse, K.; Polomski, R. E.; Wedding, D. L.; Winter, W. J. Process Development of 5-Fluoro-3-[3-[4-(5-methoxy-4-pyrimidinyl)-1-piperazinyl]propyl]-1H-indole Dihydrochloride. *Org. Process Res. Dev.* **1997**, *1*, 300−310.
(15) (a) The central experiments were added to provide a measurement of pure experimental error and to check for curvature, but not included in model analysis for screening DoEs. (b) It usually takes three or four experiments at the central point.
(16) As BNB is very corrosive to the skin, a 1/4-fraction factorial design (2^{5-2}) was generated to reduce the number of experiments.
(17) Minitab, LLC. Stepwise regression is a multiple regression analysis method provided by Minitab, which can be used to screen significance factors. Please see: Using stepwise regression and best subsets regression. Minitab 21 support. https://support.minitab.com/en-us/minitab/21/help-and-how-to/statistical-modeling/regression/supporting-topics/basics/using-stepwise-regression-and-best-subsets-regression/#what-is-stepwise-regression (last accessed September 9, 2022).
(18) Kuethe, J. T.; Tellers, D. M.; Weissman, S. A.; Yasuda, N. Development of a Sequential Tetrahydropyran and Tertiary Butyl Deprotection: High-Throughput Experimentation, Mechanistic Analysis, and DOE Optimization. *Org. Process Res. Dev.* **2009**, *13*, 471−477.
(19) (a) The significance of LOF indicates the model has a poor fit to the data, and the significance of curvature indicates the lack of square term, both suggesting that a RSM should be performed. (b) As curvature of the screening DoE model was significant, which indicated the ranges of the selected factor was close to the optimal range (assuming that the curvature is pronounced near the top of the mountain), there is no need for "path of steepest ascent" to determine the optimal range of process parameters, and they could be directly used in the RSM.
(20) If temperature was included in the RSM DoE, contour plots of BNB and DIPEA at different temperatures were possible to be generated. This can help us better understand how the process attributes change according to different temperatures. In addition, the identified factors would be further verified by the evaluation by RSM DoE, alleviating the concern of mis-interpretation or incorrect conclusions. Even if the factor temperature had not been included in the RSM DoE, the results would not have been affected.
(21) The significance of factors can also be observed in the main effect plot. The steeper the curve, the more significant the factor is.
(22) Lehrich, F.; Hopf, H.; Grunenberg, J. The Preparation and Structures of Several Cross-Conjugated Allenes ("Allenic Dendralenes"). *Eur. J. Org. Chem.* **2011**, *2011*, 2705−2718.
(23) Li, Y.; Chen, J. Y.; Qiu, R. H.; Wang, X.; Long, J.; Zhu, L.; Au, C.-T.; Xu, X. Cesium hydroxide-catalyzed Isomerization of Terminal Alkynes for the Synthesis of O-allenes and N-allenes. *Tetrahedron Lett.* **2015**, *56*, 5504−5507.
(24) (a) Zlota, A. A. Recommendations for Effective and Defendable Implementation of Quality by Design. *Org. Process Res. Dev.* **2022**, *26*, 899−914. (b) If the *p*-value threshold was set to 0.15, four parameters would be identified as "statistically significant". This would be inappropriate based on the concept of "factor sparsity". As such, the *p*-value threshold was set to 0.10 in step 3, and three parameters were selected for the RSM study.
(25) (a) Lin, K. Y.; Chen, L.; Zhou, W. H.; Lyu, X.; Ding, S.; Li, H.; Chen, H.; Jiang, Z.; Wang, Y.; Diao, W.; Liu, N. Method For Preparing Linagliptin. Chinese Patent CN106478629, 2017. (b) Li, Z.; Ge, J.; Zhang, S.; Li, J.; Wang, L.; Wang, J. Preparation of Linagliptin, Analog and Intermediate Thereof. Chinese Patent CN106554354, 2017.
(26) Guo, J. Y.; Zhai, Z. H.; Wang, L.; Wang, Z. Y.; Wu, J.; Zhang, B. Y.; Zhang, J. B. Dynamic and Thermodynamic Mechanisms of TFA Adsorption by Particulate Matter. *Environ. Pollut.* **2017**, *225*, 175−183.
(27) The content of impurity **A** and impurity **B** was obtained by testing commercially available products manufactured by Boehringer Ingelheim, Germany.
(28) BNB is a very toxic compound, and the protection effect of ordinary gloves is poor. Protective equipment and thick rubber gloves should be worn in the process of feeding, taking sample for HPLC and post-treatment even if it was used in small scale.

https://doi.org/10.1021/acs.oprd.2c00230
Org. Process Res. Dev. 2022, 26, 3254−3264